Numerical Model for the Tissue Ablation by an Excimer Laser

Luc Schnell

February 15, 2018
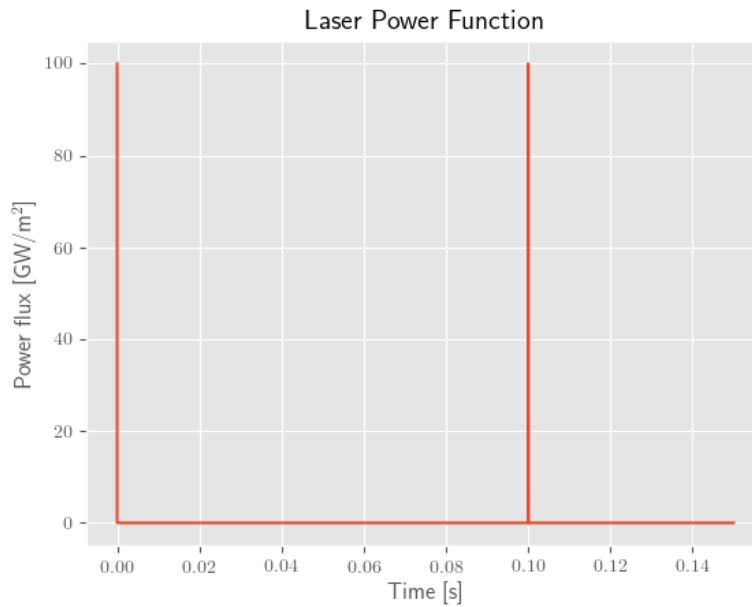
This work is based on [1].

1 Methods

1.1 Physical Model

1.1.1 Setup

An eximer laser operating at a wavelength of 213 nm is modeled. The power flux output of the laser is assumed to take the form of a step function.

The pulse duration is 8 ns, the pulse period is 0.1 s (pulse repetition rate of 10 Hz). The maximum power flux is 100 GW/m². The materials air, water and corneal tissue are present in the model. The laser radiation is only absorbed by the corneal tissue (the radiation absorbed by the 8 µm thick water film can be neglected, since the absorption coefficient of water is only on the order of 0.1 cm^{-1} for UV radiation at 213 nm [3]). The absorption coefficient for corneal tissue at 210 nm amounts to 2317 cm^{-1} (average taken from [4]).

For the parameters ρ, c and k, the following values were used:

Material	Density ρ [kg/m³]	Heat capacity c [J/(kg K)]	Heat diffusivity k [m²/s]
Air	1.177	1005	0.0262
Water	988	4180	0.644
Corneal Tissue	1062	3740	0.53

1.1.2 One-dimensional heat equation

The physical model is based on the one-dimensional heat equation

$$\rho c \frac{\partial T}{\partial t}(x,t) = k \frac{\partial^2 T}{\partial x^2}(x,t) + S(x,t), \tag{1}$$

where ρ is the density of the material, c the heat capacity (for constant pressure), k the heat diffusivity and S the laser power per unit volume. S is given by

$$S(x,t) = \mu_a(x,t) \cdot \phi(x,t), \tag{2}$$

where μ_a is the absorption coefficient of the absorbing material and ϕ is the power of the incident laser light per unit area. The power flux ϕ can be found using Beer's law:

$$\phi(x,t) = \phi_0(t) \cdot e^{-\mu_a x}, \tag{3}$$

assuming that only the material $x \geq 0$ is absorbing. Since in general the parameters k, ρ, c and μ_a are time-dependent, the one-dimensional heat equation can only be solved numerically.

1.2 Numerical Method

This section is based on [2].

There are several discretization schemes that can be implemented to find numerical solutions to the model described above. Although there exists an explicit scheme that requires the least amount of computational steps, it imposes the condition

$$\Delta t < \frac{\rho c (\Delta x)^2}{2k} \tag{4}$$

on the discretization time steps Δt for the solution to be physically realistic. This can be a strong limitation if a large timespan should be covered by the model. In these cases, the more CPU-intensive fully implicit model becomes favorable, since larger Δt can be chosen while still obtaining physically realistic solutions.
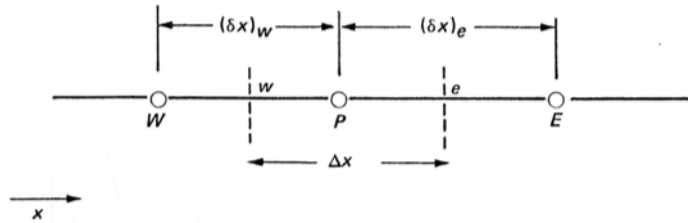
1.2.1 Fully implicit scheme

Figure 1: Grid points in the fully implicit scheme.

In the fully implicit scheme, the equation

$$a_P^0 T_P = a_E^0 T_E + a_W^0 T_W + b^0 \tag{5}$$

with

$$a_E^0 = \frac{k_E^0}{(\delta x)_e},$$

$$a_W^0 = \frac{k_W^0}{(\delta x)_w},$$

$$\alpha_P^0 = \frac{\rho^0 c^0 \Delta x}{\Delta t},$$

$$b^0 = S_P^0 \Delta x + \alpha_P^0 T_P^0,$$

$$a_P^0 = a_E^0 + a_W^0 + \alpha_P^0$$

needs to be solved for every point P in the spacial grid going from t to $t + \Delta t$. The superscript 0 stands for parameters calculated based on the "old" temperatures at time t (Δx and δx are constant in time, therefore the superscript is omitted). The subscripts E, P and W show at which points the parameters are evaluated (see Figure 1). Expression (5) results in a linear system of equations

$$\begin{pmatrix} b_1^0 \\ b_2^0 \\ b_3^0 \\ \vdots \\ b_N^0 \end{pmatrix} = \begin{pmatrix} a_{P_1}^0 & -a_{E_1}^0 & 0 & 0 & \cdots & 0 & 0 & 0 \\ -a_{W_2}^0 & a_{P_2}^0 & -a_{E_2}^0 & 0 & \cdots & 0 & 0 & 0 \\ 0 & -a_{W_3}^0 & a_{P_3}^0 & -a_{E_3}^0 & \cdots & 0 & 0 & 0 \\ \vdots & \vdots & \vdots & \vdots & & \vdots & \vdots & \vdots \\ 0 & 0 & 0 & 0 & \cdots & 0 & -a_{W_N}^0 & a_{P_N}^0 \end{pmatrix} \begin{pmatrix} T_1 \\ T_2 \\ T_3 \\ \vdots \\ T_N \end{pmatrix} \tag{6}$$

describing the "new" temperatures T_i for every point in the spacial grid at $t+\Delta t$. To solve this linear system of equations, a professional algorithm (for example Python's numpy.linalg.solve) can be used. The temperatures at the grid points 1 and N (first and last grid point) were always set back to ambient temperature to model open boundaries. Once the temperatures at $t+\Delta t$ are known, the parameters k, ρ, c and μ_a can be updated. In a last step, the power flux ϕ for all grid points based on the new values for μ_a can be found recursively via

$$\phi_{i+1} = \phi_i \cdot e^{-\mu_a \Delta x}. \tag{7}$$

1.2.2 Step sizes

The step sizes Δt and Δx do not have to be constant across the discretization grid. A suitable variation in the step sizes makes it possible to resolve fine structures (such as the short laser pulses) while being economical with computer resources. The function that was used to determine the step sizes Δx for a given x is displayed below.

Listing 1: Step sizes Δx (Python code)

```python
def delta_x(x):
    return max(0.1 * 10**(-6), min(0.1 * abs(x), 10.*10**(-6)))
```

The minimum step size 0.1 µm is taken for $|x| < 1$ µm, the maximum step size 10 µm for $|x| > 100$ µm and in between the step size is increasing linearly with x.

The function for the step sizes Δt is a bit more involved.

Listing 2: Step sizes Δt (Python code)

```python
lp = 8.0 * 10**(-9) #Laser pulse duration [s]
lpp =  0.1 #Laser pulse period (time between two pulses) [s]

def mod_t(t):
  while(t < 0):
    t += lpp
  while(t - lpp >= 0):
    t -= lpp
  return t

def delta_t(t):
  if(mod_t(t + lp) <= 3*lp):
    return lp/10.
  else:
    step = lpp/5. * abs(sin((lpp - mod_t(t))/ lpp * pi))
    while(mod_t(t) > lpp/2.0 and mod_t(t + step) < lpp/2.0):
      step /= 2.0
    return step
```

The function *mod_t* returns the time t modulo the time between two laser pulses (*lpp*) to know where we are in the periodic laser pulse cycle (step function). The function *delta_t* then returns the step size Δt depending on *mod_t(t)*. In the time interval starting one laser pulse duration (*lp*) before the actual laser pulse and ending one *lp* after the laser pulse, the step size Δt is chosen to be a tenth of the laser pulse duration (*lp/10*). Outside this interval, Δt is basically chosen according to a |sin| function that has period *lpp* and zeros for the starting times of the laser pulses. Since the laser pulse duration *lp* is very short, the code needs to make sure that the laser pulse is not "missed" (too large step size Δt that simply "jumps" over the laser pulse interval). This is resolved by the while-loop at the end of above code listing: the step size is decreased before the next laser pulse starts.

2 Results

2.1 Single Laser Pulse

Figure 2 shows $T(x, t_0)$ for different times t_0 after a single laser pulse. Note that the times t_0 in the plot increase exponentially. The distributions get flatter over time, the one with the highest peak corresponds to t = 0.008 µs (right after the laser pulse), the flattest one to t = 65536 µs.
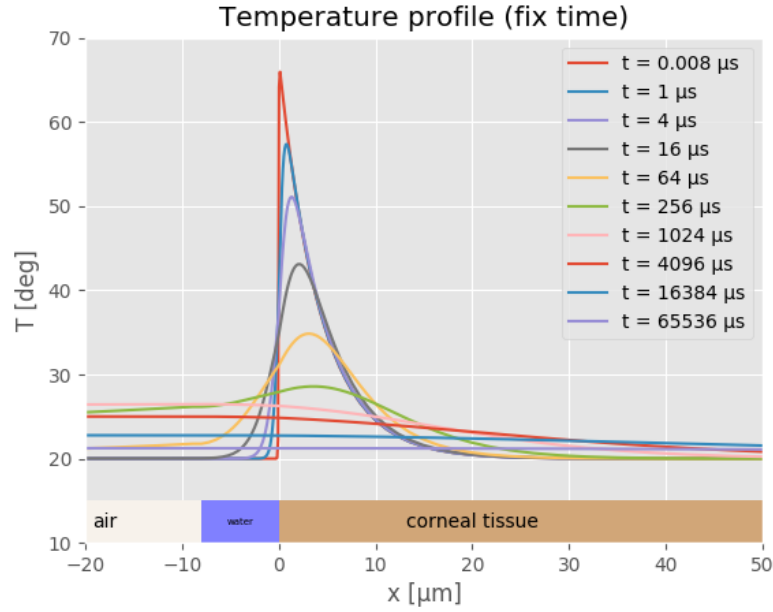

Figure 2: Temperature distributions after a single laser pulse.

2.2 Several Laser Pulses

In the upper diagram of Figure 3, $T(x, t_0)$ is displayed again, but this time for fixed t_0 immediately after the laser pulses. The temperature profiles are dominated by the power distribution of the incoming laser radiation and are thus confined to a small region. There was no time for heat conductance to flatten out the curves after the last laser pulse. Finally, the lower diagram in Figure 3 shows $T(x_0, t)$ for fixed positions x_0.
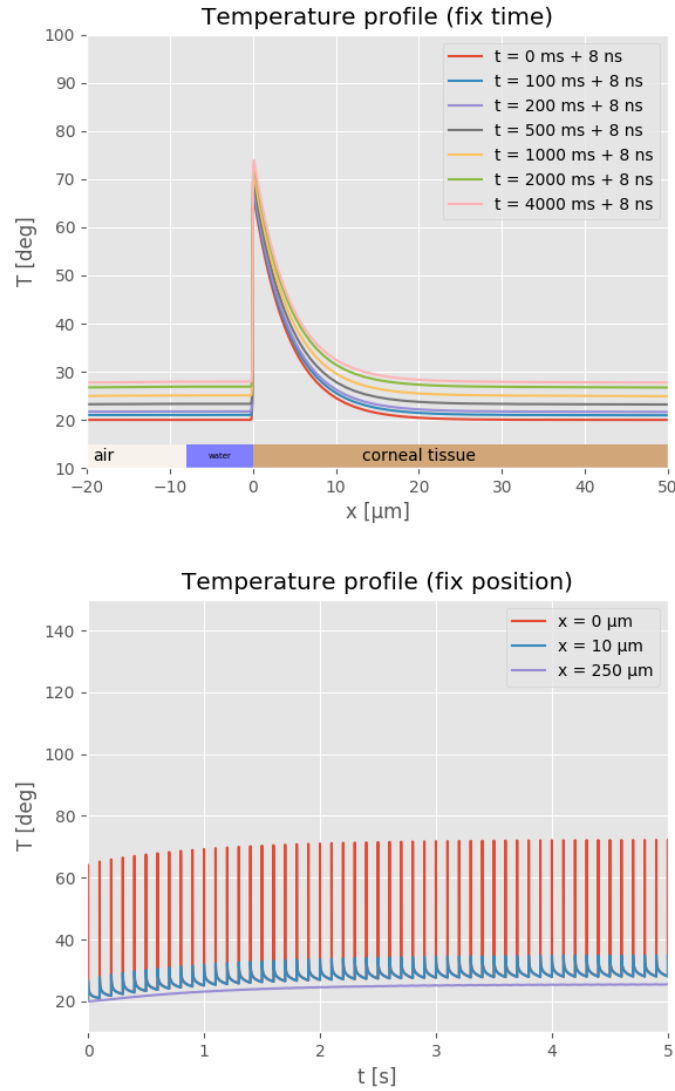
Figure 3: Temperature distribution after several consecutive laser pulses.

References

[1] Asshauer, T.: *Photoablation biologischer Weichgewebe mit gütegeschalteten Erbium-Lasern.* Institut für Angewandte Physik, Rheinische Friedrich-Wilhelms-Universität Bonn, 1992.

[2] Patankar, S.V.: *Numerical Heat Transfer and Fluid Flow.* University of Minnesota, McGraw-Hill Book Company.

[3] Smith, R.C. and Baker, K.S.: *Optical properties of the clearest natural waters (200 - 800 nm.* University of California at San Diego, Visibility Laboratory SIO. Received July 28, 1980.

[4] Lembares, A., Hu, X.-H. and Kalmus, G.W.: *Absorption Spectra of Corneas in the Far Ultraviolet Region.* Departments of Physics and Biology, East Carolina University, Greenville, North Carolina. Accepted January 14, 1997.